Volume 17, Number 4, 2024. pp. 395-402

Jordan Journal of Physics

ARTICLE

Solution of the Woods-Saxon Potential and its Application for Study of Thermodynamic Properties

Derar Altarawneh[a], **Abdullah Atef Shukri**[b] and **Akpan N. Ikot**[c,d]

[a] *Department of Applied Physics, Tafila Technical University, Tafila, 66110, Jordan.*
[b] *Department of Physics, Yarmouk University, Irbid, Jordan.*
[c] *Theoretical Physics Group, Department of Physics, University of Port Harcourt, Port Harcourt, Nigeria.*
[d] *Western Caspian University, Baku, Azerbaijan.*

Doi: **https://doi.org/10.47011/17.4.2**

Received on: 20/11/2022; *Accepted on: 26/04/2023*

Abstract: This work presents an exact analytical solution for the Schrödinger equation with the Woods-Saxon potential. To achieve this, the factorization method is utilized with the Pekeris approximation applied to the centrifugal potential for arbitrary l states. The resulting solution provides both the wave functions of the potential expressed in the hypergeometric function and the energy eigenvalues. Additionally, the study calculates the thermodynamic properties of the Woods-Saxon potential in its classical limit, including the vibrational partition function, mean vibrational energy, vibrational specific heat, vibrational mean free energy, and vibrational entropy.

Keywords: Woods-Saxon Potential, Schrodinger equation, Thermodynamic properties, Factorization method.

PACS numbers: 11.15.Ha, 12.38.Gc.

Introduction

The Schrödinger equation is a crucial tool for investigating quantum mechanical systems and making predictions. Since it encodes all the necessary information about these systems, particularly in physics and chemistry, its solution has attracted considerable interest [1, 2, 3, 4]. However, exact solutions are only feasible for a small number of potentials, prompting the development of approximation methods for tackling complex cases, such as those involving arbitrary angular momentum quantum numbers l. Several such methods have been proposed, including the factorization method [5, 6], the asymptotic iteration method [7, 8, 9], the super-symmetric quantum mechanics approach [10, 11], the Nikiforov-Uvarov method, and the factorization method [12]. The factorization method involves transforming a second-order homogeneous linear differential equation into a hypergeometric equation using appropriate transformations. In this study, we employ the factorization method to determine the nonrelativistic energy states of the standard Woods-Saxon potential [13].

The Woods-Saxon potential is a widely used short-range potential in nuclear, particle, and atomic physics that has contributed significantly to the field's development over the past several decades. This potential has been instrumental in the understanding of numerous experimental observations, including proton scattering and neutron interactions with heavy nuclei. Additionally, it is a popular model for systems of

Corresponding Author: Derar Altarawneh **Email**: derar@ttu.edu.jo

confined particles within a potential well enclosed by a potential barrier, such as protons and neutrons in atomic nuclei, electrons in metals, and nuclear fusion and fission. Researchers have shown considerable interest in solving the Schrödinger equation for the Woods-Saxon potential, with numerous studies conducted to determine the associated wave function and energy states [7, 9, 13, 14, 15, 16, 17, 18, 19, 20,21]. Studying thermodynamic functions has also garnered much attention in the last few decades, with researchers utilizing various methods to evaluate the thermodynamic properties of physical systems under different potentials [22, 23, 24].

This paper focuses on the study of the Schrödinger equation with the Woods-Saxon potential, specifically for an arbitrary angular momentum quantum number l, using the factorization method. The aim is to obtain energy levels and wave functions and subsequently apply the canonical partition function in the classical limit to analyze the thermodynamic properties of nonrelativistic particles. The paper is organized into several sections. Section I provides an introduction to the topic. Section II presents the energy states and wave function of the Woods-Saxon potential. Section III covers the thermodynamic properties of the potential, including free energy, specific heat, mean energy, and entropy. The discussion and conclusion of the paper are presented in Sections IV and V, respectively.

Energy States and Wave Function of Woods-Saxon Potential

The standard Woods-Saxon potential [1] is defined as:

$$V(r) = -\frac{V_0}{1+\exp(\frac{r-R_0}{a})}, a \ll R_0. \quad (1)$$

Here, V_0 represents the potential well depth, a is the surface thickness of the nucleus, and R_0 is the nuclear radius.

The radial part of the Schrodinger equation is:

$$\frac{d^2\psi(r)}{dr^2} + \frac{2m}{\hbar^2}[E_{nl} - V(r) - \frac{l(l+1)\hbar^2}{2mr^2}]\psi(r) = 0 \quad (2)$$

By substituting the Woods-Saxon potential, the Schrodinger equation becomes:

$$\frac{d^2\psi(r)}{dr^2} + \frac{2m}{\hbar^2}[E_{nl} + \frac{V_0}{1+\exp(\frac{r-R_0}{a})} - \frac{l(l+1)\hbar^2}{2mr^2}]\psi(r) = 0 \quad (3)$$

The equation cannot be analytically solved for $l \neq 0$, leading to the use of the Pekeris approximation to address this limitation. This approach enables the expression of the centrifugal term as:

$$\frac{l(l+1)\hbar}{2mr^2} = \alpha[S_0 + \frac{S_1}{1+exp(\frac{r-R_0}{a})} + \frac{S_1}{(1+exp(\frac{r-R_0}{a}))^2}], \quad (4)$$

where

$$\frac{l(l+1)\hbar}{2mR_0^2} = \alpha \quad (5)$$

By using Taylor expansion around $r = R_0$, the values of S_0, S_1, and S_2 are found to be:

$$\left.\begin{aligned} S_0 &= 1 - \frac{4a}{R_0} + \frac{12a^2}{R_0^2} \\ S_1 &= \frac{8a}{R_0} - \frac{48a^2}{R_0^2} \\ S_2 &= \frac{48a^2}{R_0^2} \end{aligned}\right\} \quad (6)$$

The solution presented in this study focuses on the point where the Woods-Saxon potential weakens and higher-order terms are not considered. The Woods-Saxon potential has a short range, which means that the expansion presented above is applicable only to low-energy states. With this in mind, Eq. (3) can be written as:

$$\psi''(z) + \frac{[1-2z]}{[z(1-z)]}\psi'(z) + \frac{\epsilon^2+\chi^2 z-\gamma^2 z^2}{z(z-1)^2}\psi(z) = 0 \quad (7)$$

Here, we insert the Pekeris approximation into the equation and we change the variables $r \rightarrow z$ by applying the mapping function $z = (1 + e^{\frac{r-R_0}{a}})^{-1}$. The parameters ϵ,χ, and γ are defined as:

$$\left.\begin{aligned} \epsilon^2 &= \frac{2ma^2}{\hbar^2}[E_{nl} - \alpha S_0] \\ \chi^2 &= \frac{2ma^2}{\hbar^2}[V_0 - \alpha S_1] \\ \gamma^2 &= \frac{2ma^2\alpha S_2}{\hbar^2} \end{aligned}\right\} \quad (8)$$

By using the boundary conditions of the wave functions $\psi(z)$, we obtain:

$$\left.\begin{aligned} &\psi(z) \rightarrow 0 \quad \text{when} \quad z \rightarrow 1 \\ &\psi(z) \rightarrow 0 \quad \text{when} \quad z \rightarrow 0 \end{aligned}\right\} \quad (9)$$

Thus, we can write the wave function as:

$$\psi(z) = z^{\mu}(1-z)^{\phi}f(z) \quad (10)$$

By substituting Eq. (10) into Eq. (7), we obtain the following equation:

$$z(1-z)f''(z)+[1+2\mu-(2\mu+2\phi+2)z]f'(z)-[(\mu+\phi)^2+(\mu+\phi)-\gamma^2]f(z)+[\frac{-\epsilon^2+\mu^2}{z(1-z)}+\frac{\phi^2-\mu^2+\chi^2-\gamma^2}{1-z}]f(z)=0 \tag{11}$$

Equation (10) becomes a Gauss hypergeometric equation if and only the following equations vanish:

$$-\epsilon^2+\mu^2=0 \text{ and } \phi^2-\mu^2+\chi^2-\gamma^2=0 \tag{12}$$

Equation (11) becomes:

$$z(1-z)f''(z)+[1+2\mu-(2\mu+2\phi+2)z]f'(z)-[(\mu+\phi+\tfrac{1}{2}+\sqrt{\tfrac{1}{4}+\gamma^2})((\mu+\phi+\tfrac{1}{2}-\sqrt{\tfrac{1}{4}+\gamma^2})]f(z)=0 \tag{13}$$

Equation (13) is compared with the hypergeometric differential equation which has the following form:

$$z(1-z)f''(z)+[c-(a+b+1)z]f'(z)-abf(z)=0 \tag{14}$$

We find that:

$$\left.\begin{aligned} a &= \mu+\phi+\tfrac{1}{2}+\sqrt{\tfrac{1}{4}+\gamma^2} \\ b &= \mu+\phi+\tfrac{1}{2}-\sqrt{\tfrac{1}{4}+\gamma^2} \\ c &= 1+2\mu \end{aligned}\right\} \tag{15}$$

With the help of the Gauss hypergeometric function, a solution to Eq. (14) is given by:

$$f(z)={}_2F_1(a,b;c;z)=\frac{\Gamma(c)}{\Gamma(a)\Gamma(b)} \tag{16}$$

By substituting Eqs. (15) and (16) into Eq. (10), the wave function becomes:

$$\psi(z)=z^{\mu}(1-z)^{\phi}{}_2F_1(a,b;c;z) \tag{17}$$

The hypergeometric function appearing in Eq. (16) can be reduced into a polynomial of degree n when either a or b equals a negative integer $-n$. Under this condition, the wave function can asymptotically vanish.

$$\left.\begin{aligned} \mu+\phi+\tfrac{1}{2}+\sqrt{\tfrac{1}{4}+\gamma^2} &= -n \\ \mu+\phi+\tfrac{1}{2}-\sqrt{\tfrac{1}{4}+\gamma^2} &= -n \end{aligned}\right\} \tag{18}$$

By using Eqs. (12) and (18), one can find the non-relativistic energy spectrum as:

$$E_{nl}=\frac{-\hbar^2}{2ma^2}[\frac{(\omega-n)}{2}-\frac{(\gamma^2-\chi^2)}{2(\omega-n)}]^2+\alpha S_0 \tag{19}$$

where

$$\omega=((\sqrt{\tfrac{1}{4}+\gamma^2}-\tfrac{1}{2}) \tag{20}$$

Using Eqs. (8) and (9), one can get:

$$\epsilon=\frac{1}{2}[(\omega-n)+\frac{\gamma^2-\chi}{(\omega-n)}] \tag{21}$$

Since for the bound states ($\epsilon>0$), one can get that $(\omega-n)>0$ and $\omega\neq n$. Here, the index n is a non-negative integer and describes the quantization of the bound states and the energy spectrum. This result shows a perfect agreement with previous results

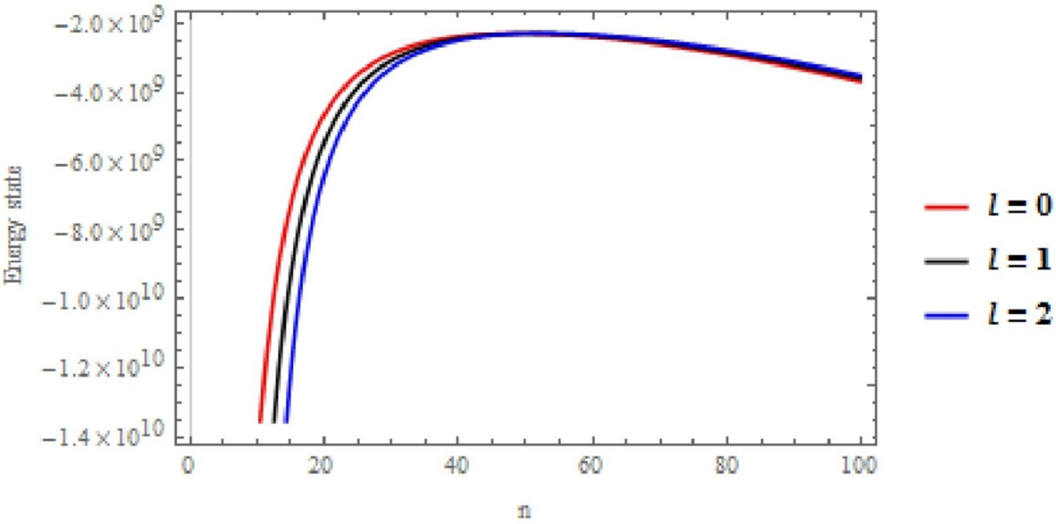

FIG. 1. Energy states (eV) versus radial quantum number (n) for different values of l.

Thermodynamic Properties

For studying the thermodynamic properties of the Woods-Saxon potential, we first obtain the vibrational partition function which is defined as:

$$Z_{vib}(\beta) = \sum_{n=0}^{\lambda} e^{-\beta E_{nl}} \tag{22}$$

where $\beta = 1/k_b T$, k_b is the Boltzmann constant, and λ is the upper-bound vibrational quantum number. At high temperature T (classical limit) the sum can be converted to an integral. By substituting the energy state, one can find:

$$Z_{vib}(\beta) = \int_0^{\lambda} e^{-\beta E_{nl}}\, dn = \frac{1}{2}\sqrt{b\beta}\left(2\sqrt{\pi}\left(\operatorname{erfi}\left(\frac{\sqrt{b\beta}}{\lambda}\right)+1\right) - \frac{2\lambda e^{\frac{b\beta}{\lambda^2}}}{\sqrt{b\beta}}\right) e^{\beta\left(c+P(\omega-n)^2\right)} \tag{23}$$

where:

$$\operatorname{erfi}(x) = \frac{\mathrm{erf(x)}}{i} = \frac{2}{\pi}\int_0^{x} e^{t^2}\, dt \tag{24}$$

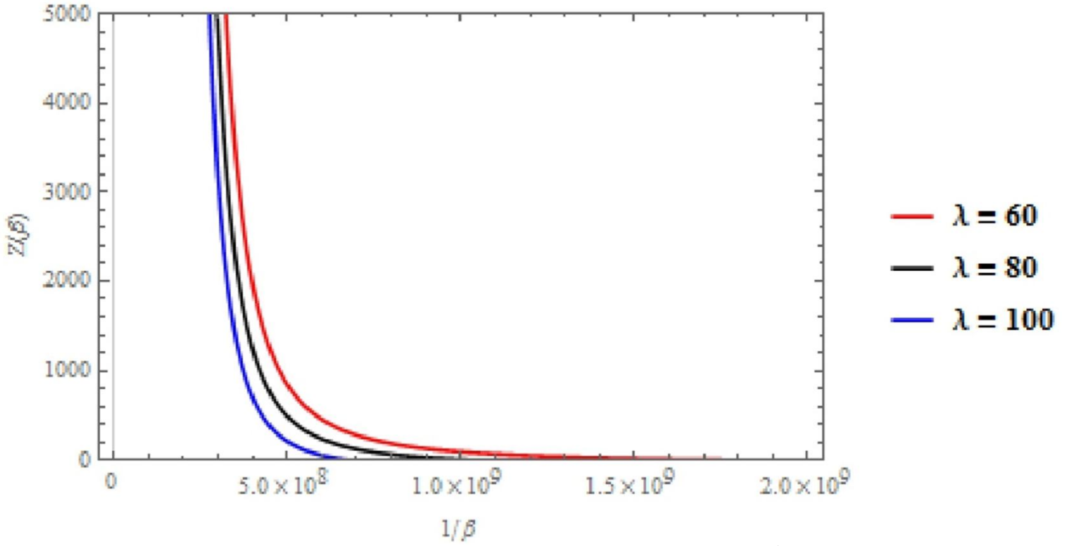

FIG. 2. Vibrational partition function Z versus $\frac{1}{\beta}$.

Having determined the vibrational partition function, we can easily obtain the thermodynamic properties for the Woods-Saxon as follows:

1. The Vibrational Mean Energy U:

$$U(\beta) = -\frac{\partial}{\partial\beta}\ln Z_{vib}(\beta) \tag{25}$$

After substituting Eq. (22) into Eq. (25), the vibrational mean energy will have the form:

$$U(\beta) = -\frac{2e^{-\beta(c+P(\omega-n)^2)}\left(\frac{b\left(2\sqrt{\pi}\left(\operatorname{erfi}\left(\frac{\sqrt{b\beta}}{\lambda}\right)+1\right)-\frac{2\lambda e^{\frac{b\beta}{\lambda^2}}}{\sqrt{b\beta}}\right)e^{\beta(c+P(\omega-n)^2)}}{4\sqrt{b\beta}}\right)}{\sqrt{b\beta}\left(2\sqrt{\pi}\left(\operatorname{erfi}\left(\frac{\sqrt{b\beta}}{\lambda}\right)+1\right)-\frac{2\lambda e^{\frac{b\beta}{\lambda^2}}}{\sqrt{b\beta}}\right)}$$

$$+\frac{2e^{-\beta(c+P(\omega-n)^2)}\left(\frac{1}{2}\sqrt{b\beta}\left(2\sqrt{\pi}\left(\operatorname{erfi}\left(\frac{\sqrt{b\beta}}{\lambda}\right)+1\right)-\frac{2\lambda e^{\frac{b\beta}{\lambda^2}}}{\sqrt{b\beta}}\right)(c+P(\omega-n)^2)e^{\beta(c+P(\omega-n)^2)}+\frac{\lambda e^{\frac{b\beta}{\lambda^2}+\beta(c+P(\omega-n)^2)}}{2\beta}\right)}{\sqrt{b\beta}\left(2\sqrt{\pi}\left(\operatorname{erfi}\left(\frac{\sqrt{b\beta}}{\lambda}\right)+1\right)-\frac{2\lambda e^{\frac{b\beta}{\lambda^2}}}{\sqrt{b\beta}}\right)} \tag{26}$$

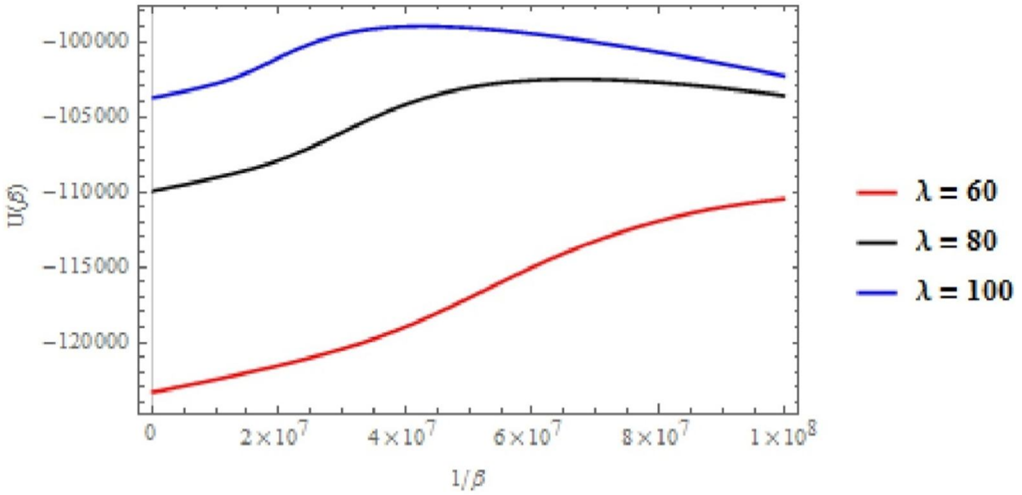

FIG. 3. Mean vibrational energy $U(cm^{-1})$ versus $\frac{1}{\beta}(K)$ for different values of λ.

2. *Mean Free Energy F*:

$$F=-\frac{1}{\beta}\ln Z_{vib}(\beta)=-\frac{\log\left(\frac{1}{2}\sqrt{b\beta}\left(2\sqrt{\pi}\left(\operatorname{erfi}\left(\frac{\sqrt{b\beta}}{\lambda}\right)+1\right)-\frac{2\lambda e^{\frac{b\beta}{\lambda^2}}}{\sqrt{b\beta}}\right)e^{\beta(c+P(\omega-n)^2)}\right)}{\beta} \tag{27}$$

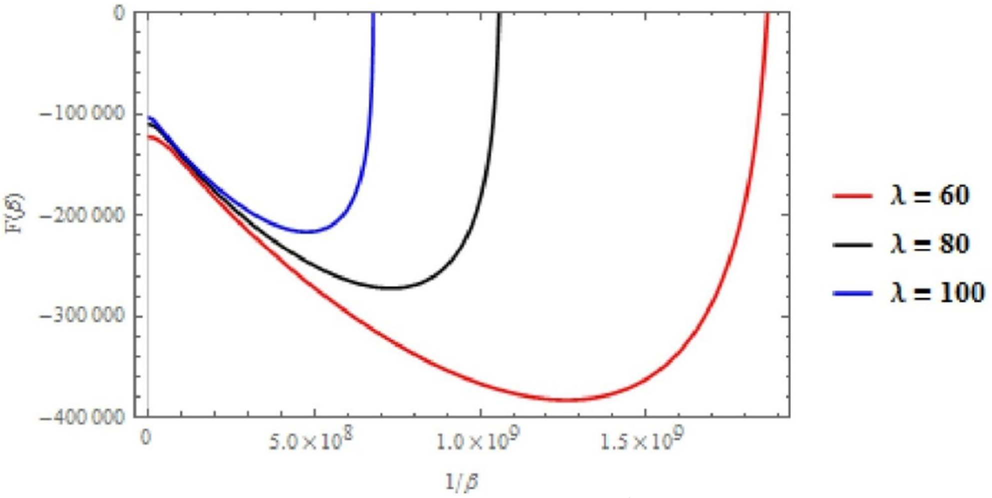

FIG. 4. Mean vibrational free energy $F(cm^{-1})$ versus $\frac{1}{\beta}(K)$ for different values of λ.

3. *Vibrational Specific Heat C*:

$$C=-K_b\beta^2\frac{\partial}{\partial\beta}U$$

$$C=-K_b\beta^2\frac{\partial}{\partial\beta}U$$

$$C=-\beta^2\left(\frac{be^{-\beta\left(P(\omega-n)^2+c\right)}\left(\frac{e^{\left(P(\omega-n)^2+c\right)\beta+\frac{b\beta}{\lambda^2}}\lambda}{2\beta}+\frac{be^{\beta\left(P(\omega-n)^2+c\right)}\left(2\sqrt{\pi}\left(\operatorname{erfi}\left(\frac{\sqrt{b\beta}}{\lambda}\right)+1\right)-\frac{2e^{\frac{b\beta}{\lambda^2}}\lambda}{\sqrt{b\beta}}\right)}{4\sqrt{b\beta}}-\frac{1}{2}\sqrt{b\beta}e^{\beta\left(P(\omega-n)^2+c\right)}\left(P(\omega-n)^2+c\right)\left(2\sqrt{\pi}\left(\operatorname{erfi}\left(\frac{\sqrt{b\beta}}{\lambda}\right)+1\right)-\frac{2e^{\frac{b\beta}{\lambda^2}}\lambda}{\sqrt{b\beta}}\right)\right)}{(b\beta)^{3/2}\left(2\sqrt{\pi}\left(\operatorname{erfi}\left(\frac{\sqrt{b\beta}}{\lambda}\right)+1\right)-\frac{2e^{\frac{b\beta}{\lambda^2}}\lambda}{\sqrt{b\beta}}\right)}\right)$$

$$+\beta^2\left(\frac{2e^{-\beta\left(P(\omega-n)^2+c\right)}\left(-P(\omega-n)^2-c\right)\left(\frac{e^{\left(P(\omega-n)^2+c\right)\beta+\frac{b\beta}{\lambda^2}}\lambda}{2\beta}+\frac{be^{\beta\left(P(\omega-n)^2+c\right)}\left(2\sqrt{\pi}\left(\operatorname{erfi}\left(\frac{\sqrt{b\beta}}{\lambda}\right)+1\right)-\frac{2e^{\frac{b\beta}{\lambda^2}}\lambda}{\sqrt{b\beta}}\right)}{4\sqrt{b\beta}}-\frac{1}{2}\sqrt{b\beta}e^{\beta\left(P(\omega-n)^2+c\right)}\left(P(\omega-n)^2+c\right)\left(2\sqrt{\pi}\left(\operatorname{erfi}\left(\frac{\sqrt{b\beta}}{\lambda}\right)+1\right)-\frac{2e^{\frac{b\beta}{\lambda^2}}\lambda}{\sqrt{b\beta}}\right)\right)}{\sqrt{b\beta}\left(2\sqrt{\pi}\left(\operatorname{erfi}\left(\frac{\sqrt{b\beta}}{\lambda}\right)+1\right)-\frac{2e^{\frac{b\beta}{\lambda^2}}\lambda}{\sqrt{b\beta}}\right)}\right)$$

$$\left. +\beta^2\left(\beta^2 k_b\left(\frac{be^{-\beta\left(P(\omega-n)^2+c\right)}\left(\frac{e^{\left(P(\omega-n)^2+c\right)\beta+\frac{b\beta}{\lambda^2}}\lambda}{2\beta}+\frac{be^{\beta\left(P(\omega-n)^2+c\right)}\left(2\sqrt{\pi}\left(\operatorname{erfi}\left(\frac{\sqrt{b\beta}}{\lambda}\right)+1\right)-\frac{2e^{\frac{b\beta}{\lambda^2}}\lambda}{\sqrt{b\beta}}\right)}{4\sqrt{b\beta}}-\frac{1}{2}\sqrt{b\beta}e^{\beta\left(P(\omega-n)^2+c\right)}\left(P(\omega-n)^2+c\right)\left(2\sqrt{\pi}\left(\operatorname{erfi}\left(\frac{\sqrt{b\beta}}{\lambda}\right)+1\right)-\frac{2e^{\frac{b\beta}{\lambda^2}}\lambda}{\sqrt{b\beta}}\right)\right)}{(b\beta)^{3/2}\left(2\sqrt{\pi}\left(\operatorname{erfi}\left(\frac{\sqrt{b\beta}}{\lambda}\right)+1\right)-\frac{2e^{\frac{b\beta}{\lambda^2}}\lambda}{\sqrt{b\beta}}\right)}\right)\right)\right)$$

$$+\beta^2\left(\frac{2e^{-\beta\left(P(\omega-n)^2+c\right)}\left(-P(\omega-n)^2-c\right)\left(\frac{e^{\left(P(\omega-n)^2+c\right)\beta+\frac{b\beta}{\lambda^2}}\lambda}{2\beta}+\frac{be^{\beta\left(P(\omega-n)^2+c\right)}\left(2\sqrt{\pi}\left(\operatorname{erfi}\left(\frac{\sqrt{b\beta}}{\lambda}\right)+1\right)-\frac{2e^{\frac{b\beta}{\lambda^2}}\lambda}{\sqrt{b\beta}}\right)}{4\sqrt{b\beta}}-\frac{1}{2}\sqrt{b\beta}e^{\beta\left(P(\omega-n)^2+c\right)}\left(P(\omega-n)^2+c\right)\left(2\sqrt{\pi}\left(\operatorname{erfi}\left(\frac{\sqrt{b\beta}}{\lambda}\right)+1\right)-\frac{2e^{\frac{b\beta}{\lambda^2}}\lambda}{\sqrt{b\beta}}\right)\right)}{\sqrt{b\beta}\left(2\sqrt{\pi}\left(\operatorname{erfi}\left(\frac{\sqrt{b\beta}}{\lambda}\right)+1\right)-\frac{2e^{\frac{b\beta}{\lambda^2}}\lambda}{\sqrt{b\beta}}\right)}\right)$$

$$-\beta^2\left(\frac{2e^{\frac{b\beta}{\lambda^2}-\beta\left(P(\omega-n)^2+c\right)}\lambda\left(\frac{e^{\left(P(\omega-n)^2+c\right)\beta+\frac{b\beta}{\lambda^2}}\lambda}{2\beta}+\frac{be^{\beta\left(P(\omega-n)^2+c\right)}\left(2\sqrt{\pi}\left(\operatorname{erfi}\left(\frac{\sqrt{b\beta}}{\lambda}\right)+1\right)-\frac{2e^{\frac{b\beta}{\lambda^2}}\lambda}{\sqrt{b\beta}}\right)}{4\sqrt{b\beta}}-\frac{1}{2}\sqrt{b\beta}e^{\beta\left(P(\omega-n)^2+c\right)}\left(P(\omega-n)^2+c\right)\left(2\sqrt{\pi}\left(\operatorname{erfi}\left(\frac{\sqrt{b\beta}}{\lambda}\right)+1\right)-\frac{2e^{\frac{b\beta}{\lambda^2}}\lambda}{\sqrt{b\beta}}\right)\right)}{b\beta^2\left(2\sqrt{\pi}\left(\operatorname{erfi}\left(\frac{\sqrt{b\beta}}{\lambda}\right)+1\right)-\frac{2e^{\frac{b\beta}{\lambda^2}}\lambda}{\sqrt{b\beta}}\right)^2}\right) \tag{28}$$

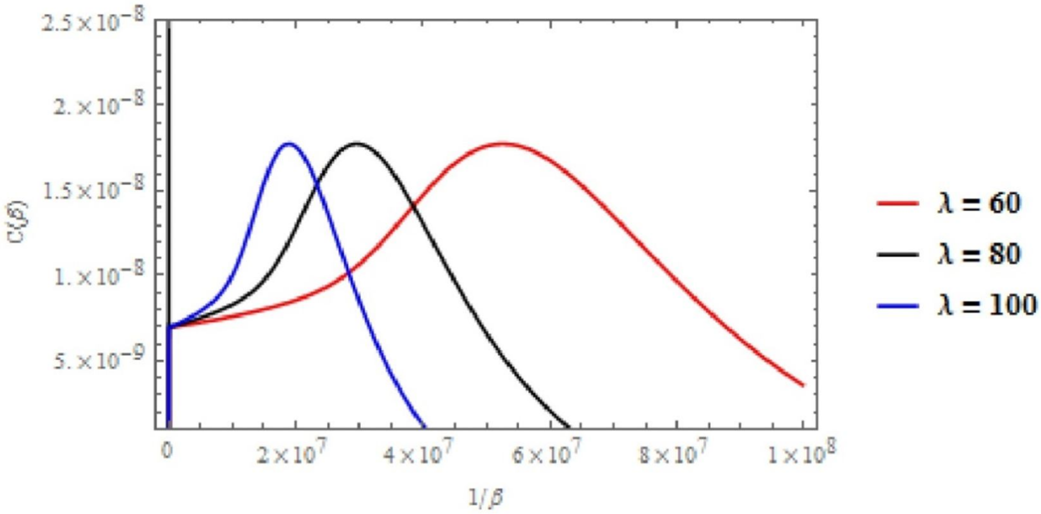

FIG. 5. Vibrational specific heat capacity $C(cm^{-1}K^{-1})$ versus $\frac{1}{\beta}(K)$ for different values of λ.

4. *The Vibrational Entropy S:*

$$S=k_b\beta^2\frac{\partial}{\partial\beta}F=\beta^2k_b\left(\frac{\log\left(\frac{1}{2}\sqrt{b\beta}\left(2\sqrt{\pi}\left(\operatorname{erfi}\left(\frac{\sqrt{b\beta}}{\lambda}\right)+1\right)-\frac{2\lambda e^{\frac{b\beta}{\lambda^2}}}{\sqrt{b\beta}}\right)e^{\beta\left(c+P(\omega-n)^2\right)}\right)}{\beta^2}\right)$$

$$-\beta^2k_b\left(\frac{2e^{-\beta(c+P(\omega-n)^2)}\left(\frac{b(2\sqrt{\pi}(\operatorname{erfi}(\frac{\sqrt{b\beta}}{\lambda})+1)-\frac{2\lambda e^{\frac{b\beta}{\lambda^2}}}{\sqrt{b\beta}})e^{\beta(c+P(\omega-n)^2)}}{4\sqrt{b\beta}}\right)}{\beta\sqrt{b\beta}(2\sqrt{\pi}(\operatorname{erfi}(\frac{\sqrt{b\beta}}{\lambda})+1)-\frac{2\lambda e^{\frac{b\beta}{\lambda^2}}}{\sqrt{b\beta}})}\right)$$

$$+\beta^2k_b\left(\frac{2e^{-\beta(c+P(\omega-n)^2)}\left(\frac{1}{2}\sqrt{b\beta}(2\sqrt{\pi}(\operatorname{erfi}(\frac{\sqrt{b\beta}}{\lambda})+1)-\frac{2\lambda e^{\frac{b\beta}{\lambda^2}}}{\sqrt{b\beta}})(c+P(\omega-n)^2)e^{\beta(c+P(\omega-n)^2)}+\frac{\lambda e^{\frac{b\beta}{\lambda^2}+\beta(c+P(\omega-n)^2)}}{2\beta}\right)}{\beta\sqrt{b\beta}(2\sqrt{\pi}(\operatorname{erfi}(\frac{\sqrt{b\beta}}{\lambda})+1)-\frac{2\lambda e^{\frac{b\beta}{\lambda^2}}}{\sqrt{b\beta}})}\right) \tag{29}$$

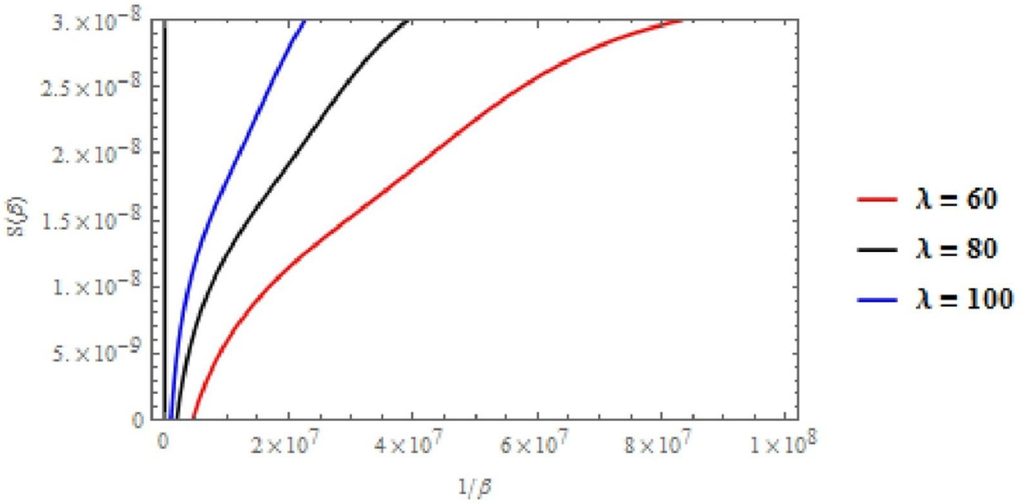

FIG. 6. Vibrational entropy $S(cm^{-1}K^{-1})$ versus $\frac{1}{\beta}(K)$ for different values of λ.

The study focused on the Woods-Saxon potential, with energy states calculated first, followed by the determination of the vibrational partition function at high temperatures. From this, various thermodynamic properties were derived using specific values for parameters including $\hbar = 6.582119 \times 10^{-16}\, eV.s$, $k_b = 8.6177 \times 10^{-5} \frac{eV}{K}$, $m = 51amu$, $V_0 = 2300Mev$, $R = 1.285fm$, $1cm = 1.2398 \times 10^{-4}eV$, and $a = 0.65fm$. Figure 1 displays the relationship between energy states and temperature for different l values. This figure illustrates that the energy spectrum approaches zero as n values increase. The second figure, labeled as Fig. 2, demonstrates that the vibrational partition function of the Woods-Saxon potential drps considerably after $\frac{1}{\beta} = 1 \times 10^8$ for all values of λ. This partition function serves as a foundation for evaluating a range of thermodynamic properties. Another figure, Fig. 3, displays the alteration of the vibrational free energy of the Woods-Saxon potential. Additionally, the internal energy of the potential is linear across all λ values until $\frac{1}{\beta} = 4 \times 10^7$, which matches the vibrational specific heat capacity in Fig. 5. In Fig. 4, the vibrational mean free energy decreases with temperature until it reaches a minimum value. Figure 5 shows that the vibrational specific heat capacity rises as temperature increases until it reaches a peak and then has a concave ascent until it reaches saturation. Finally, Fig. 6 displays the vibrational entropy for the Woods-Saxon potential. At low temperatures, the entropy is small, but it approaches infinity at very high temperatures.

Conclusion

Using the factorization method, the Schrödinger equation for the standard Woods-Saxon potential was solved, yielding eigenvalues and corresponding eigenfunctions in terms of hypergeometric functions. The results were found to agree perfectly with previous studies. In addition, the thermodynamic properties of the system were analyzed, including vibrational mean energy, vibrational free energy, vibrational specific heat capacity, and vibrational entropy. These properties were determined using the high-temperature vibrational partition function and were obtained within the classical limit. The behaviors of all the thermodynamic functions are presented through various plots.

References

[1] Woods, R.D. and Saxon, D.S., Phys. Rev., 95 (1954) 577.

[2] Schrödinger, E., Ann. Phys., 385 (1926) 437.

[3] Schrödinger, E., Ann. Phys., 384 (1926) 489.

[4] Oyewumi, K.D., J. Math. Chem., 50 (2012) 1039.

[5] Mir-Kasimov, R.M., Phys. Part. Nuclei, 44, (2013) 422.

[6] Pahlavani, H.R.M. and Ghezelbash, M., J. Microphys., 3 (2013) 1.

[7] Ikhdair, S.M., Falaye, B.J., and Hamzavi, M., Chin. Phys. Lett., 30 (2013) 020305.

[8] Ciftci, H., Hall, R.L., and Saad, N., J. Phys. A: Math. Gen., 36 (2003) 11807.

[9] Falaye, B.J., Hamzavi, M., and Ikhdair, S.M., Chin. Phys. Lett., 30 (2013) 020305.

[10] Ikot, A.N., Obong, H.P., Abbey, T.M., Zare, S., Ghafourian, M., and Hassanabadi, H., Few-Body Syst., 57 (2016) 807.

[11] Liang, H., Shen, S., Zhao, P., and Meng, J., Phys. Rev., C87 (2013) 014334.

[12] Jia, Y., Eur. Phys. J. D, 71 (2017) 3.

[13] Kumar, P.R. and Wong, B.R., AIP Conf. Proc., 1657 (2015) 160001.

[14] Badalov, V.H., Ahmadov, H.I., and Ahmadov, A.I., Int. J. Mod. Phys. E, 18 (2009) 631.

[15] Berkdemir, C., Berkdemir, A., and Sever, R., Phys. Rev., C72 (2005) 027001.

[16] Lütfüoğlu, B.C., Eur. Phys. J. Plus, 133 (2018) 309.

[17] Lütfüoğlu, B.C., Commun. Theor. Phys., 69 (2018) 23.

[18] Lütfüoğlu, B.C., Commun. Theor. Phys., 71 (2019) 267.

[19] Lütfüoğlu, B.C., Can. J. Phys., 96 (2018) 843.

[20] Lütfüoğlu, B.C., Lipovský, J., and Kříž, J., Eur. Phys. J. Plus, 133 (2018) 17.

[21] Lütfüoğlu, B. C., Akdeniz, F., and Bayrak, O., J. Math. Phys., 57 (2016) 032103.

[22] Pacheco, M.H., Landim, R.R., and Almeida, C.A.S., Phys. Lett., A311 (2003) 93.

[23] Pacheco, M.H., Maluf, R.V., Almeida, C.A.S., and Landim, R.R., EPL, 108 (2014) 10005.

[24] Yahya, W.A. and Oyewumi, K.J., J. Assoc. Arab Univ. Basic Appl. Sci., 21 (2016) 53.